Chapter 2

Background

Chemical and Physical Properties of Ice and Snow

2.1 Physical Properties of ice/snow

2.1.1 Ice Fundamentals

Ice in its various crystalline morphologies consists of interconnected water molecules with an elemental composition of 2:1 of hydrogen and oxygen. The molecular arrangement for a single water molecule is shown below in Figure 1.[1]

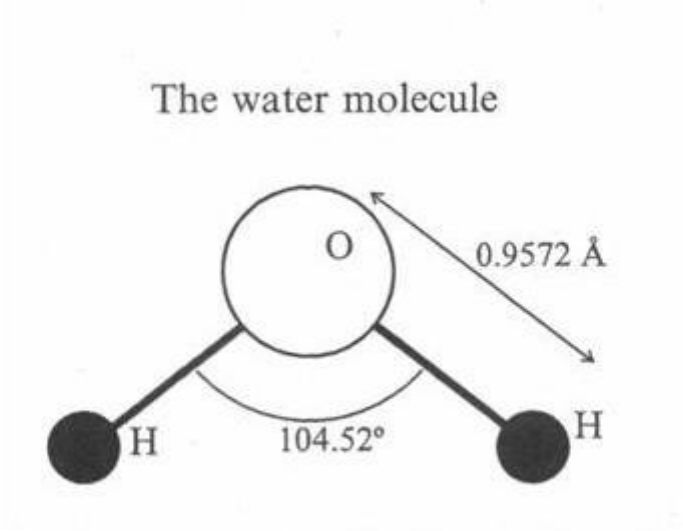

Figure 2.1. The geometry of a free H_2O molecule.[1]

The near tetrahedral bond angle defines the bent configuration of water and determines its degree of accommodation in a crystalline structure. Furthermore, the bent configuration induces an electric dipole moment, which is the result of an asymmetrical distribution of electronic charge due to the electronegativity of the oxygen.

Water has several unique characteristics in that it forms by far the most distinctly different solid phases of any identified matter.[2] For instance, between ~ 273 and 193 K water vapor deposited on a surface forms a crystalline solid with hexagonal symmetry, known as *hexagonal ice* or *ice* I_h. This structure was the first high-pressure phase of ice to

be identified.[3] The deposition of water vapor on a base between ~ 193 and 143 K yields a cubic crystalline ice structure, referred to as *cubic ice* or *ice* I_c. This mode of ice is a metastable form of *ice* I_h. Below ~ 133 K, when water vapor is allowed to settle on a surface, the accumulation is called *vitreous* or *amorphous ice*, consisting of either a noncrystalline glass or very small crystals. Moreover, there are eleven other high-pressure phases of ice (ices **II-XII**) that are commonly acknowledged as *high pressure polymorphs of ice*.

2.1.2 Elastic, Thermal, and Lattice Vibrational Properties

2.1.2a Elasticity

An uncomplicated representation of a crystalline solid, such as ice, displays the atoms as point masses connected by coils. The coils are stretched or compressed and the network is deformed when the arrangement is subjected to an external stress. This deformation comprises an elastic strain.

For an elastic distortion of ice, the stress, σ, as a product of the strain, ε, and the elastic modulus E, is given in following equation:

$$\sigma = E\varepsilon \tag{1}$$

However, this simple treatment neglects the tensile stress, which causes both an extension and a lateral contraction given by $v\varepsilon$, where v is Poisson's ratio. Although the tensor expressions can describe the elastic deformation of anistropic materials (e.g., single ice crystals), the matrix formulation can also be utilized.

In matrix notation, the elastic properties of ice are characterized by the following six equations:

$$\varepsilon_i = \sum_{j=1}^{6} s_{ij}\sigma_j \tag{2}$$

or by the inverse suite of equations:

$$\sigma_i = \sum_{j=1}^{6} c_{ij}\varepsilon_j, \tag{3}$$

where c_{ij} and s_{ij} are termed the *elastic constants* or *stiffness* and the *elastic compliances*, respectively. It is apparent that the stresses and strains each have six components σ_i and ε_i that are distinct with respect to the axis of the crystal. Hexagonal crystals have five autonomous compliances:

$$s_{11} = s_{22},$$

$$s_{33},$$

$$s_{12} = s_{21},$$

$$s_{13} = s_{31} = s_{23} = s_{32},$$

$$s_{44} = s_{55},$$

and

$$s_{66} = 2(s_{11} - s_{12}).$$

The equivalence relationships between c_{ij} and s_{ij} are described extensively by Nye *et al*.[4]

The elastic constants c_{11} and c_{12} or s_{11} and s_{12} are frequently chosen for isotropic materials, such as polycrystalline ice. The shear modulus, G, and the bulk modulus, K, describe how isotropic materials resist changes in volume and shape. In terms of the elastic compliances, G and K are defined as follows:

$$G = \frac{1}{2(s_{11} - s_{12})} \tag{4}$$

$$K = \frac{1}{3(s_{11} - 2s_{12})} \tag{5}$$

2.1.2b Thermal Characteristics

Figure 2.2 illustrates molar heat capacity C_p/R vs. temperature at constant pressure.

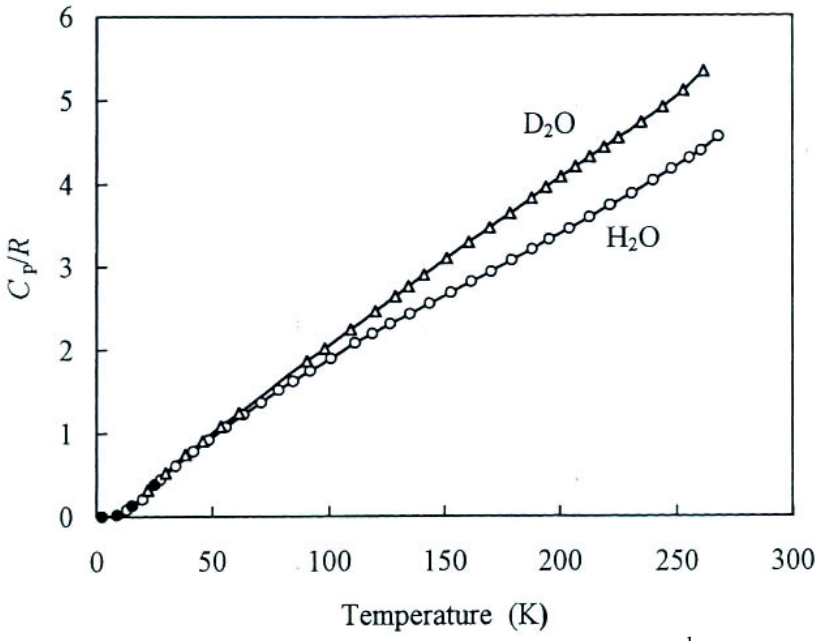

Figure 2.2. Adapted from Petrenko and Whitworth.[1] Molar heat capacity of ice at constant pressure C_p versus temperature. D_2O data from Matsuo *et al*.[5] H_2O data from Haida *et al*.,[6] where temperature values (solid circles) are from Flubacher *et al*.[7]

For H_2O at the lowest temperatures, C_p/R fluctuates as T^3, while at higher temperatures the mass of the hydrogen atom is the crucial factor causing an increase in molecular motion and thus considerable excitation of modes. This is reflected in the larger heat capacity of D_2O compared to H_2O.

Heat expansivity also needs to be considered when describing the thermal properties of ice. Data on the thermal expansion of ice shows that the process is isotropic. The lattice parameters of H_2O and D_2O are used to calculate their respective mean linear expansion coefficents $\alpha(T)$.[8] Moreover, the mode of thermal expansion is dependent on the anharmonic nature of the inter-atomic forces of a particular crystalline phase.[9,10]

Thermal conductivity measurements on ice show that there is no anisotropy[11-13] and that the conductivity above 60 K is given by the relationship:

$$\lambda = \frac{651\, W\, m^{-1}}{T}, \tag{6}$$

where W is watts.

2.1.2c Lattice Vibrational Properties

A crystal matrix of *'n'* H_2O molecules consists of 3*n* atoms that exert forces on each other. This arrangement, therefore, exhibits $3 \times 3n$ normal modes of vibration. Three techniques have been used to gain information about the frequency of these modes in ice. They are infrared absorption, Raman spectroscopy, and inelastic neutron scattering. The spectra acquired from these techniques depend on the density of states of the vibrational modes in ice.

Ice is translucent in the visible and near infrared, but its absorption rises for wavelengths $\lambda \geq 1300$ nm. The permittivity of H_2O ice decreases as the square of the refractive index for visible light, from 3.16 to 1.70, when passing through the frequency range of the infrared absorption bands. The reduction in permittivity is due to the minute dislocations of atoms from their equilibrium positions in an electric field, which cause an enhancement in the electrical polarizability of ice. Infrared absorption data for H_2O ice in the frequency range 30 - 4000 cm^{-1} is given by Bertie *et al*.[14]

Raman spectroscopy entails the use of a beam of monochromatic light (e.g., from a laser) to pass through a sample, where the scattered light is analyzed to form a spectrum. Spectra *actually* represent frequency-shifts of low-intensity components by the quanta required to excite appropriate modes of vibration in the lattice. Raman spectral data on polycrystalline ice is provided by Wong and Whalley.[15,16]

Inelastic neutron scattering involves the use of a mono-energetic beam of neutrons of near-thermal energy to pass through a sample. The scattered neutrons' energy distribution is then determined as a function of the scattering angle. Li *et al*.[17] and Li[18] present the most recent data on neutron scattering of H_2O ice.

2.1.3 Electrical Properties

Several processes occur when an electric field is applied to an ice specimen. First, the movement of electrons in relation to the nuclei and small distortions of molecules under restoring forces cause single molecules to become polarized. Second, the reorientation of bonds or molecules induces polarization within ice, and third, current, which flows according to Ohm's law in ice, is due to the movement of protons,[19] which can be measured with appropriate electrophysical devices.

The electric polarization, *P,* for processes 1 and 2 is related to the electric field *E* through the equation

$$P = \varepsilon_o \chi E, \tag{7}$$

where ε_o is the 'permittivity of free space' and χ the electric susceptibility. The current density, *J*, for process 3 is given by the following

$$J = \sigma_s E, \tag{8}$$

where σ_s is the steady-state conductivity. Both of these characteristics are anistropic in ice I_h.

A specified Debye relaxation process can describe how polarization in a material (e.g., process 2 above) moves toward equilibrium. This mode of Debye relaxation behaves in accordance with the following equation:

$$\frac{dP}{dt} = \frac{1}{\tau_D}(P_s - P), \tag{9}$$

where τ_D, which is dependent on the purity of ice and temperature, is termed the Debye relaxation time and $P_s = \varepsilon_o \chi_s E$.

In both ice and liquid water the static permittivities, ε_s are similar and are due to the dipole moment of the water molecule, which exists in both liquid and ice water. The primary difference is τ_D, the time scale for polarization to occur (i.e., for liquid water at 10 ^oC $\tau_D \approx 1.2 \times 10^{-11}$ s and for water ice at -11 ^oC $\tau_D \approx 5.0 \times 10^{-5}$ s). This ~ 6 order of magnitude difference arises from the fact that water molecules in ice are *fixed* in the lattice, whereas water molecules in liquid water are in dynamic motion.

The above theory pertains to the thermal equilibrium polarization of an arrangement of molecules in an applied electric field. However, ice crystals deviate from the theoretical representation since ice rules are strictly followed and equilibrium is never achieved. Bjerrum[20] recognized that polarization and conduction occur in ice if defects exist that deviate locally from the ice rules. These defects, which are called *protonic point defects*, allow the reorientation of molecules along their path and, in essence, alter a particular molecular configuration from one form into another. Therefore, the mobility and concentration of such defects determine the Debye relaxation time.

There are four kinds of protonic point defects specific to ice-like structures: *L*- and *D-defect* (*Bjerrum defects*);[21] H_3O^+ and OH^- (*ionic defects*) which presumably arise from the self-dissociation of water in the QLL domains followed by diffusion back into the crystalline matrix. Figure 2.3 shows how protons and hydroxide ions are accomodated in the ice structure.

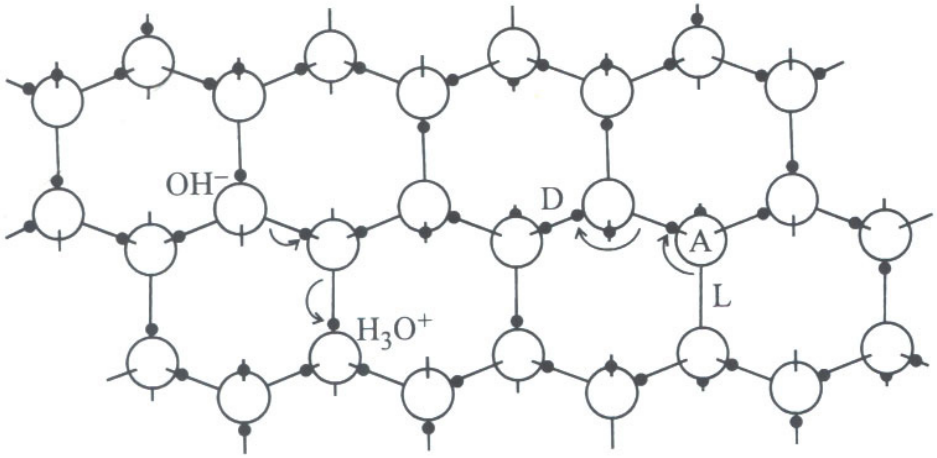

Figure 2.3. Adapted from Petrenko and Whitworth.[1] Bjerrum and ionic defects introduced into an a layer of ice structure projected on the $(10\bar{1}0)$ plane.

In addition, Bjerrum defects arise when a single molecule (i.e., A as shown in Figure 2.3) is turned into a new orientation and produces one bond with two protons pointing towards each other and another bond with no protons. To rectify this unstable scenario, neighboring molecules undergo additional turns to disconnect the flawed bonds. In this scheme ionic defects are created from the transfer of a proton from one molecule to a neighboring molecule. The transfer process is divided by consecutive jumps of protons from one end of a hydrogen bond to another. The movement of both the Bjerrum and ionic defects follow a zig-zag course along suitably oriented bonds in a crystal, while bonds and molecules in their path are reoriented. These defects bear effective charges of magnitudes e_{DL} (Bjerrum defects) and $e_{\pm}$ (ionic defects). Moving a proton of charge e is equivalent to the net effect of moving a D- and H_3O^+ defect along a path. The charge properties of the Bjerrum and ionic defects are given in the following equations:

$$e_{DL} + e_{\pm} = e, \tag{10}$$

$$e_{H_3O^+} = -e_{OH^-} = e_{\pm}, \tag{11}$$

$$e_D = -e_L = e_{DL}, \tag{12}$$

2.1.4 Diffusion Through Ice

There are five categories of point defects in ice that describe the movement of atoms or molecules from one site to the next: molecular defects, protonic defects, ionic or atomistic impurities, electronic defects, and combined defects.[1] Molecular defects involve the displacement of entire H_2O molecules, leaving a vacancy (region where a molecule is absent from its usual site) or an interstitial (an extra molecule occupying a site in a cavity). Protonic defects entail the two ionic and Bjerrum defects. Impurity atoms involve the substitition of one atom for another. Electronic defects involve the behavior of ionized molecules or trapped electrons. Combined defects entail the occurrence of two or more of either the molecular defects, protonic defects, impurity atoms or ions, and electronic defects. Point defects can travel to an adjacent site via thermal activation. Bjerrum defects move from one site to another by the rotation of a water molecule, whereas ion defects travel by the skipping of a proton along a hydrogen bond. Interstitials can just hop into a neighboring site, while for vacancies a molecule leaves a new site vacant after hopping into a vacant site. The amount of jumps made by a particular defect per second is given by the following Arrhenius equation

$$v_h = v \exp\left(-\frac{E_m}{K_B T}\right), \tag{13}$$

where v = the order of frequency of vibration of the defect in the potential well and E_m = the height of the barrier. For a particular point defect traveling in a one-dimensional potential of period a the diffusion coefficient D is defined as

$$D = a^2 v_h. \tag{14}$$

Based on experimental observations[22] on ice, equation 14 is deduced to

$$D_i = D_{io} \exp\left(-\frac{E_{im}}{K_B T} \right). \tag{15}$$

D_i refers to the diffusion coefficient of a specific point defect i (e.g., for protonic defects, vacancies, and interstitials), D_{io} is the diffusion coefficient pre-factor, and E_{im} is the activation for motion.

The diffusion of isotopically-labeled molecules in ice is described by its self-diffusion coefficient; it may take place by either the interstitial or vacancy process. The interstitial and vacancy mechanism are both expected to abide by the following equation,

$$D_s = D_{so} \exp\left(-\frac{E_s}{K_B T} \right). \tag{16}$$

D_s refers to the self-diffusion coefficient, D_{so} refers to the self-diffusion pre-factor, and E_s refers to the activation energy for self-diffusion. One of the primary findings of self diffusion experiments is that self-diffusion occurs by the movement of whole molecules.[23,24]

The significance of point defects and self-diffusion to atmospheric chemistry and occurrences in the snowpack are widespread (e.g., analysis of ice cores for the reconstruction of paleoatmospheric compositions[25-29]). Atmospheric gases, which are trapped in ice as air bubbles at relatively shallow depths, are slowly transformed into clathrate hydrates at lower depths.[30,31] The dynamic process controlling the formation of various clathrates may affect the distribution and composition of atmospheric species in ice cores resulting in a variable fractionation of atmospheric air in ice cores. For

example, there are significant differences between the Vostok and Dome Fuji ice core data, which have been attributed to the faster diffusion of O_2 than N_2.[32-34] In this regard, Satoh *et al*.[35] determined that the diffusion coefficients of He, Ne, and Ar, which were ~ 10^{-9} m^2 s^{-1}, ~ 10^{-10} m^2 s^{-1}, and ~ 10^{-11} m^2 s^{-1}, respectively, between 258 and 268 K. The order of estimated diffusion coefficients appeared to be a function of their molecular radii. In addition, protons, electrons, hydroxyl radicals ($^{\cdot}OH$) and hydroxide (OH^-) ions exhibit high diffusion coefficients[36,37] in ice, while solutes, such as, nitric acid (HNO_3), hydrogen chloride (HCl), and formaldehyde (HCHO) exhibit lower diffusion coefficients.[38-46] These results have serious implications for ice core records, since the relative diffusion of major and minor impurities in ice cores may smooth their chemical profiles with depth.[25]

2.1.5 Optical Properties of Ice/Snow

Scattering and absorption are the two mechanisms by which light interacts with snow grains, where their significance is wavelength dependent. According to Warren,[47] there is minimal light absorption in the visible and UV regions, where scattering dominates, while in the near-infrared the relative extent of absorption and scattering is approximately equal. At short wavelengths (e.g., UV radiation) the effective pathlength of photons in snow will be increased by multiple scattering.

The variation of light intensity with depth is complex. In the upper few centimeters of snow, the depth-dependence of the light intensity is convoluted by the albedo (reflectivity) of the snow surface and the fact that a certain fraction of light is scattered back to the atmosphere. At lower depths, light becomes isotropic from multiple

scattering; the Bouger-Lambert Law describes the exponential variation of light with depth by

$$I(d^2) = I(d^1)e^{-k(\lambda)(d^2-d^1)}, \quad (17)$$

where $I(d^1)$ and $I(d^2)$ are light intensities at depths d^1 and d^2, respectively, and $k(\lambda)$ is the asymptotic flux extinction coefficient.

Warren has shown[47] that the optical properties of snow in the visible and IR depend on several factors including: 1) the geometry of the ice grains; 2) liquid-water inclusions; 3) snow density; and 4) the nature and concentration of the solid and soluble impurities. Warren then established that the extinction coefficients in the visible and UV range are similar;[48] thus it is possible to extrapolate extinction coefficients determined in the visible region to estimate extinction coefficients in UV region for snow/ice. In order to verify these factors, Beaglehole *et al*.[49] investigated UV to IR (350 to 900 nm) light transmittance through snow as a function of layer thickness and determined that thickness inhomogeneity may cause thicker snow layers to follow an extinction that is larger, compared to thinner snow layers, which may be due to the fact that the top 5 to 10 cm has a higher scattering coefficient. King and Simpson[50] determined that the e-folding depths in snow over the wavelength range of over 300 – 548 nm varied greatly between sampling sites, which they attributed to the variation in impurities at the sites. They[50] also suggested that ~ 85 % of the possible photochemistry occurs in the top 10 cm of a snowpack.

2.1.6 Ice Plasticity

The flow of glaciers down mountain slopes has been explained in terms of some of the specific properities of ice (e.g., ductility and brittleness).[51-53] For example, ice will

not rupture when it is slowly deformed plastically by tension or compression.[54] The importance of understanding the mechanical properties of ice are multifold. They are essential for 1) modeling the movement of of glaciers on ice sheets; 2) the proper design of structures with or on ice; 3) the effect of floating ice on drilling platforms; and 4) the construction of ice-breaking ships.

Single ice crystals are highly malleable under mild stress (e.g., ~ 0.1 to 0.5 MPa) and slow creep. For example, Glen and Perutz transformed ice rods into ribbon-shaped ice structures by applying specified strains.[55] The plasticity of single ice crystals is anisotropic,[1] but polycrystalline ice may exhibit both anisotropic[1] and isotropic[56-58] deformation.

2.1.7 Quasi-liquid layer (QLL) on Ice Surfaces and Subusrface-Subeutectic Solutions in Ice

The ice-air interface of solids is an area that exhibits characteristics different from those of the bulk material. This is primarily due to the fact that atoms (or molecules) at the surface only encounter bonding forces with other molecules from one side; simultaneoulsy, there is a similar imbalance at other interfaces. Furthermore, this behavior causes the dislocation of atoms from their original locations, alterations in their associated force and engergy constants, and effects on layers below the ice-air demarcation. Michael Faraday[59-62] in 1850 first suggested that the ice-air interface consists of a thin wet film, variously called the quasi-liquid layer (QLL), premelting layer, liquid-like layer, or surface melting layer, by showing “that a particle of water which could retain the liquid state whilst touching ice on only one side, could not retain the liquid if it were touched by ice on both sides.”

Other substances, such as solid rare gases, molecular solids, metals, and semiconductors, contain a liquid-like layer on their surfaces. The fact that the boundary between the solid and vapor phase is wetted by a thin liquid film causes the free energy of the boundary to be lower than it would be if the thin liquid film were absent.[63] In other words, if the surface of ice were initially dry, then it would reduce its interfacial free energy by converting a layer (e.g., the surface) of the solid to liquid. Hence, a liquid-like layer should exist over some limited temperature range on the surface of ice, below its bulk normal melting temperature. The existence of the QLL is not prohibited due to its thinness and closeness to the normal melting temperature of ice. The thickness (d) of the QLL is present at a state where the free energy of the ice system is at a minimum and is governed by the competition between the free energy of the ice surface and the energy required to melt a solid layer.

As shown below (eqn. 17), the free energy of the QLL per unit area, $G_{QLL}(T,P,d)$, consists of both surface and bulk terms.[63]

$$G_{QLL}(T,P,d) = [\rho_l \mu_l(T,P)]d + \gamma(d) \tag{18}$$

It is assumed here that a solid is in equilibrium with a vapor at temperature (T) and pressure (P), where ρ_l is the density potential, μ_l is the chemical potential, and $\gamma(d)$ is the interfacial coefficient $(= \Delta\gamma f(d) + \gamma_{sv})$. It follows that $\Delta\gamma = \gamma_{lv} + \gamma_{ls} - \gamma_{sv}$ and $f(d)$ is the interfacial potential, which increases from 0 to 1 as d goes from 0 to ∞. $G_{QLL}(T,P,d)$ ranges from the interfacial free energy of the dry solid-vapor interface, γ_{sv}, (at $d = 0$) to $\gamma_{lv} + \gamma_{ls}$ (at $d = \infty$); γ_{lv} and γ_{ls} are the interfacial free energy of the liquid-vapor interface and the interfacial free energy of the liquid-solid interface, respectively.

The interfacial potential $f(d)$ causes the chemical potential of the bulk solid and the QLL to be unequal, which in turn, relocates the thermodynamic coordinates from the normal phase boundary.[63] The difference in chemical potential of the solid and liquid $(\Delta\mu \equiv \mu_s - \mu_l)$, compounded with the interfacial potential $f(d)$, allows for the theoretical equation for the thickness of QLL. For dispersion or van der Waals surface forces acting at the interface $f(d) = \left(\frac{d^2}{d^2 + \sigma^2}\right)$, where σ is a normal molecular diameter, the thickness of the QLL is given by

$$d = \left(-2\sigma^2 \frac{\Delta\gamma T_o}{\rho_l q_m (T_o - T)}\right)^{1/3} \tag{19}$$

For equation 19, ρ_l is the bulk liquid density, q_m is the latent heat of melting/molecule, T represents the ambient temperature, and T_o is the normal melting temperature of the bulk solid. Dash[64] and Takagi[65] also derived the theoretical expression for the thickness (d) of the QLL in the case of short range forces:

$$d = \lambda \ln\left(-\frac{\Delta\gamma T_o}{\rho_l q_m \lambda (T_o - T)}\right), \tag{20}$$

where λ is the decay length of the short range forces.

The thickness of the QLL as a function of temperature has been quantified both experimentally[66-76] and theoretically.[77-83] With the single exception of Elbaum *et al.*[69] whose experiments were done on exposed horizontal facets in the prismatic orientation $(10\bar{1}0)$, these studies have shown that the QLL layer increases with increasing temperature. As the melting point is approached, the QLL appears to be indistinguishable from the liquid phase in its uppermost layers. However, the QLL transitions to an

apparent crystalline order within several molecular layers below the surface (1 molecular layer ~ 0.3 nm).[77-82,84] In addition, solutes accumulate in the internal water-vein system at triple junctions (three-grain intersections) and nodes (four-grain intersections).[85-87] This effect was demonstrated by Fukazawa *et al*.[87] using micro-Raman spectroscopy to analyze ice below the pore close-off depth from two Antarctic sites. In ice collected from the Nansen, Antarctic site ($-35 \leq T/^{o}C \leq -8$), NO_3^- and HSO_4^- were discovered in the quasi-liquid phase at triple-junctions, while in ice collected from the South Yamamoto site, SO_4^{2-} was found in a distinct liquid phase between −8 and −20 ^{o}C. Fukazawa *et al*.[87] concluded that Antarctic ice is a non-static environment with fluid-like domains both at the ice-air interface and deep within subsurface regions.

The thickness of the QLL is a function of both T and T_o. As stated previously, the thickness of the QLL increases with increasing temperature, approaching its limiting dimension (i.e., V/A or volume/flat surface area) as $T \to T_o$. Additionally, impurities enhance its thickness.[73,83]

The addition of impurities at constant pressure will shift the normal melting point of the bulk solid, which is directly dependent on the concentration of the impurity. As defined by Raoult's law, 'this shift' is expressed as

$$T_c = T_o\left(1 - \frac{RT_o n_i}{q_m n}\right), \tag{21}$$

where T_c is the freezing temperature, R is the gas constant, q_m is the heat of fusion of the solvent, n_i is the number of moles of solute, and n is the number of moles of solvent.

The QLL plays a pivotal role in environmental phenomena such as 1) controlling the friction of ice and snow; 2) soil freezing, permafrost formation, and frost heave; 3) sintering and sliding of glaciers, sea ice, and snow fields; and 4) behavior of atmospheric ice. For instance, the slipperiness of ice and snow imply that they are covered by a thin water film on their surfaces, which in turn reduces their coefficient of friction.[88-93] The QLL has also been suggested to contribute to the electrification of the thunder clouds via charge transfer at the liquid-ice interface.[94,95] Abbatt *et al*.[96] even proposed that polar stratospheric clouds are able to accommodate HCl by dissolution in multilayer-thick quasi-liquid films, where they can efficiently participate in ozone destruction during winter and spring months in Antarctica and the Arctic.

2.1.8 Segregation of Impurities During the Freezing of Liquid Solutions

Most solutes are too large to be molecularly incorporated within the ice lattice during the freezing of aqueous solutions.[97-105] Therefore, the majority of solutes (e.g., NO_3^-, HSO_4^-, and SO_4^{2-}) are partitioned to the quasi-liquid layer (QLL) and subsurface water channels (or veins).[85-87] The degree of ion segregation during the freezing of dilute solutions depends on the solute concentration and freezing rates.[106]

It has been known and assumed that, generally, chemical reactions occur faster in the liquid phase relative to the solid phase since the migration or diffusion of molecules is severely inhibited in the solid phase. Surprisingly, certain chemical reactions are accelerated in partially frozen aqueous solutions.[107-120] Fennema[117] described the five factors significant for acceleration: freeze concentration effect, catalytic effect of ice crystals, enhanced proton migration in ice than in water, more ideal catalyst-substrate orientation due to freezing, and greater dielectric constant for water than for ice.

Furthermore, solute cations and anions exhibit an unequal distribution in the ice and solution phase during the freezing process. This inequality induces an electric potential, also known as the "freezing potential," between the solution and the growing ice. The electrostatic force generated causes anions or cations to accumulate in the water contiguous to the interface, where the potential is neutralized by extremely mobile H_3O^+ and OH^-.[121] The pH of the solution phase changes, accordingly. For example, Takenaka *et al*.[102] showed that, compared to the liquid phase, the reaction of nitrous acid with dissolved oxygen was acclerated by a factor of ca. 10^5 by freezing. This finding was attributed mainly to the freeze concentration effect. They[102] also showed that specified salts (e.g., NaCl, KCl, Na_2SO_4, and HCl) either prevented or allowed the reaction of nitrous acid and dissolved oxygen to occur, which was a direct function of whether these salts caused a positive or negative freezing potential in the remaining liquidus or solidus. The reduction of pH in the unfrozen solution was also inferred from their results. These occurrences have direct environmental implications, such as the postulated protonation of NO_2^- in acidic snowpack regions, where after $HONO_{(g)}$ can readily be released.[122]

2.2 Nitrate in Polar Ice Sheets

2.2.1 Nitrate Abundance in Polar Ice and Its Implications

Logan[123] and Platt[124] have argued that the deposition of inorganic nitrate (e.g., gaseous HNO_3 and aerosol NO_3^-) on ice surfaces is one of the main sinks for atmospheric nitrogen oxides. If nitrate concentrations within ice cores were conserved, they would provide pertinent paleoclimatic and paleoatmospheric information. In addition, they would also provide further understanding of the nitrogen cycle in the atmosphere (e.g., how NO_x ($NO + NO_2$) mixing ratios affect the primary tropospheric oxidants, OH, HO_2,

and O_3). Simultaneoulsy, extrapolating past atmospheric conditions and further elucidating the nitrogen cycle is complicated by extremely inconsistent HNO_3 and NO_x global distributions and their respective variable source and sink trends.

At Summit, Greenland, nitrate accounts for approximately 50% and 43% of the total inorganic anions in pre-industrial and contemporary polar ice, respectively.[125] At the South Pole, nitrate accounts for about 34% of the total anions.[126]

2.2.2 Origin of Nitrate at Polar Ice Regions

There are numerous sources of nitrate to polar ice regions. These sources, originating as nitrogen oxides, are combustion of fossil fuels,[127] biomass burning,[128] N_2 fixation by lightning,[129] oxidation of NH_3,[130,131] the oxidiaton of atomic nitrogen produced during the irradiation of molecular nitrogen by galactic cosmic rays,[127] and microbrial processes in soils (e.g., soil exhalation).[132,133]

The deposition of nitrate to south polar snow is relatively small. Furthermore, there appears to be no correlation between solar activity (e.g., solar proton events and 11-year solar cycle) and measured nitrate concentrations at south polar snow-covered regions.[127] In contrast, Legrand and Kirchner[127] proposed that lightning at mid-low latitudes and NO_x generated in the lower stratosphere contributes about 33 to 50% and about 33%, respectively, to the nitrate content at south polar snow-covered regions. It was also suggested that electron fluxes may cause a greater contribution to nitrate profiles in polar snow.[134] Polar stratospheric clouds also contribute to nitrate concentrations to the polar snowpack by way of deposition. Anthropogenic emission of NO_x in the northern hemisphere also has caused greater Arctic nitrate snow concentrations than the Antarctic.[25,135]

2.2.3 Nitrate's Postdepositional Processing and Its Seasonal Deposition Cycle

Average nitrate levels in polar ice cores range from 20 to 80 ng g^{-1} (0.45 to 1.78 μM), where surface-snow has been known to contain up to 300 ng g^{-1} (6.70 μM).[136] The Vostok ice-core nitrate record illustrates clearly near-surface increases, which have been attributed to post-depositional processing and redistribution within the snowpack.[137] A multitude of other[136-140] studies have illustrated the rapid loss of nitrate at the snow-surface within just days of deposition; nitrate at the snow-surface is reduced less rapidly (e.g., a few years) in areas that experience lower accumulation rates. Still, the mechanisms governing nitrate's postdepositional behavior is still under debate. Legrand *et al*.[141] suggested, for example, that post-depositional loss of nitrate is likely limited in the presence of high concentrations of mineral dust, and that significant scavenging of HNO_3 by mineral dust occurs based on the observation showing coincident elevated levels from glacial periods of nitrate in Antarctic ice[141] and at the High Qinghai-Tibetan Plateau[142] with mineral dust concentrations. Other proposed mechanisms include: volatilization of HNO_3, scavenging of nitrate by wind-blown gases or particles, photochemical destruction of nitrate, and the blowing of wind on the snow/ice surface.

Regardless of the post-depositional processing of nitrate, ice core measurements have shown that NO_3^- exhibits a seasonal cycle.[143] Certain time frames in nitrate's ice core records bare remnance to specific sources. For example, Legrand *et al*.[141] deduced that nitrate maximums between spring to summer are due to stratospheric inputs and a peak in late winter is due to sedimentation of polar stratospheric clouds. On the other hand, Greenland ice core records consistently show a summer peak in nitrate levels, which may be caused by the thermal decomposition of peroxyacetyl nitrate (PAN).[140]

2.3 Nitrate Photochemistry and Related Chemical Processes in Ice

2.3.1 Nitrate Photochemistry in the Aqueous Phase

The photochemistry of nitrate in the aqueous phase has been studied extensively.[144-149] Dissolved nitrate has two primary absorption bands in the UV. The first occurs in the far UV via the strong $\pi \rightarrow \pi^*$ transition, centered at 201 nm (ε_{max} = 9500 M^{-1} cm^{-1}), and the second is a weaker absorption band that occurs via the highly forbidden $n \rightarrow \pi^*$, centered at 302 nm (ε_{max} = 7.14 M^{-1} cm^{-1}). Furthermore, it was proposed that the weaker absorption band may occur from the combination of a singlet and triplet $n \rightarrow \pi^*$ and $\sigma \rightarrow \pi^*$ transition.[150,151]

Mack and Bolton[149] showed that the overall stoichiometry for nitrate irradiation is

$$NO_3^- \xrightarrow{h\nu} NO_2^- + {}^1/_2 O_2. \qquad (22)$$

In the absence of $^{\cdot}OH$ scavengers this stoichiometry is maintained over the entire pH range.[152,153] For $\lambda < 280$ nm, the major reaction pathway is through the isomerization of $[NO_3^-]^*$, generated via reaction 23, to form $ONOO^-$, peroxynitrite, and at low pH, peroxynitrous acid, HOONO (eqn. 24). HOONO can also be produced from the recombination of OH and NO_2 within a solvent cage as shown in reaction 25. HOONO isomerizes rapidly back to NO_3^- (eqn. 26).[149]

$$NO_3^- \xrightarrow{h\nu} [NO_3^-]^* \qquad (23)$$

$$[NO_3^-]^* \longrightarrow ONOO^- + H^+ \longrightarrow HOONO \qquad (24)$$

$$OH + NO_2 \longrightarrow HOONO \qquad (25)$$

$$HOONO \longrightarrow NO_3^- + H^+ \qquad (26)$$

At $\lambda > 300$ nm, photolysis of nitrate in aerated aqueous solutions at pH < 6 has been shown to have two primary photolytic pathways as shown in reactions 27 and 28. O^- readily hydrolyzes to form OH and OH^- (eqn. 29).

$$[NO_3^-]^* \longrightarrow NO_2^- + O(^3P) \qquad \phi \sim 1\times10^{-3} \qquad (27)$$

$$[NO_3^-]^* \longrightarrow NO_2 + O^- \qquad \phi \sim 1\times10^{-3} \qquad (28)$$

$$O^- + H_2O \longrightarrow OH + OH^- \qquad (29)$$

Atomic oxygen produced in reaction 27 can react with molecular oxygen ($[O_2]_{water} \sim 0.3$ mM) via reaction 30 or with nitrate by way of reaction 31 at $[NO_3^-] \geq 5$ mM.[145]

$$O_2 + O(^3P) \longrightarrow O_3 \qquad k_{30} \approx 4.0\times10^9\ M^{-1}\ s^{-1} \qquad (30)$$

$$NO_3^- + O(^3P) \longrightarrow NO_2^- + O_2 \qquad k_{31} = 2.24\times10^8\ M^{-1}\ s^{-1} \qquad (31)$$

According to Hoigne *et al.*,[154] ozone, which is generated by reaction 30, is either consumed by reaction with NO_3^- (eqn. 32) or by decomposition to $^{\cdot}OH$.[154,155]

$$NO_2^- + O_3 \longrightarrow NO_3^- + O_2 \qquad k_{32} = 3.7\times10^5\ M^{-1}\ s^{-1} \qquad (32)$$

The UV absorption spectrum of nitrite displays three absorption bands: the first peak is at 220 nm, and the latter two peaks are maxima at 318 nm ($\varepsilon_{max} = 10.90\ M^{-1}\ cm^{-1}$) and 354 nm ($\varepsilon_{max} = 22.90\ M^{-1}\ cm^{-1}$). Analogous to NO_3^-, nitrite undergoes direct photolysis as shown in reaction 33, to produce the hydroxyl radical. It is also oxidized subsequently by OH via reaction 34.

$$NO_2^- + H^+ \xrightarrow{hv} NO + OH \qquad \phi \sim 6\times10^{-2} \qquad (33)$$

$$NO_2^- + OH \longrightarrow NO_2 + OH^- \qquad k_{33} = 2.0\times10^{10}\ M^{-1}\ s^{-1} \qquad (33)$$

2.3.2 Nitrate Photochemistry in Ice

A number of recent studies[156-165] have shown that NO_x is produced within snowpack interstitial air and is released to the overlying boundary.[156,166-168] Based on nitrate's aqueous phase photochemistry, the release of NO and NO_2 has been attributed to the photodecomposition of nitrate. Due to the existence of the QLL[66-83] at the ice-air interface and subeutectic subsurface solution phases[85-87] in ice, the chemical reactions governing nitrate's photochemistry in the aqueous phase are extrapolated to the ice media, where nitrate photochemistry in ice is presumed to be dictated by analogous photochemical reactions. In other words, nitrate's aqueous phase photochemistry can serve as basis to assess its photochemistry in the ice phase.

Overall, the implications of nitrate photolysis are multi-fold. For instance, it has been assumed that if nitrate levels were preserved, after encapsulation within ice cores, they would provide reliable information pertaining to Earth's paleo-atmospheric composition and paleoclimate.[136,169] Therefore, nitrate photolysis could alter ice core records of other trace species (e.g., CO_2, H_2O_2, and CH_4), which would affect the elucidation of past atmospheric conditions.[136,170] In addition, NO_x and $^{\cdot}OH$ produced in snowpack interstitial air and released to the overlying boundary layer, as a result of nitrate photolysis, could greatly influence the mixing ratios of the tropospheric oxidants, O_3, $^{\cdot}OH$, and HO_2.[156,166-168] Acidic snow/ice environments should readily cause the protonation of nitrite produced during nitrate photolysis, which would enhance $^{\cdot}OH$ levels in the overlying boundary layer.[122] $^{\cdot}OH$ generated during nitrate photolysis will oxidize organic matter contained in the snowpack,[167,168] releasing products, such as formaldehyde

(HCHO) and acetaldehyde (CH_3CHO). Nitrate photochemistry may also be important in the production of NO_x in cirrus clouds since HNO_3 and NO_y is rapidly removed by cirrus clouds.[171-174] Lastly, the photolysis of nitrate may have some significance to photochemical reactions that are believed to occur on ice particles in the interstellar medium.[175-186]

References

(1) Petrenko, V. F.; Whitworth, R. W. *Physics of Ice*; University Press: Oxford, 1999.

(2) Hobbs, P. V. *Ice Physics*; Clarendon Press: Oxford, **1974**.

(3) Tammann, G. *Annalen der Physik* **1900**, *2*, 1.

(4) Nye, J. F. *Physical properties of crystals*; Clarendon Press: Oxford, **1957**.

(5) Matsuo, T.; Tajima, Y.; Suga, H. *J. Phys. Chem. Solids* **1986**, *47*, 165.

(6) Haida, O.; Matsuo, T.; Suga, H.; Seki, S. *J. Chem. Thermodyn.* **1974**, *6*, 815.

(7) Flubacher, P.; Leadbetter, A. J.; Morrison, J. A. *J. Chem. Phys.* **1960**, *33*, 1751.

(8) Rottger, K.; Endriss, A.; Ihringer, J.; Doyle, S.; Kuhs, W. F. *Acta Crystallogr. Sect. B-Struct. Commun.* **1994**, *50*, 644.

(9) Collins, J. G.; White, G. K. *Thermal expansion of solids* msterdam: North-Holland, **1964**; Vol. 4.

(10) Ashcroft, N. W.; Mermin, N. D. *Solid State Physics*; Holt, Rinehart, and Winston: New York, **1976**.

(11) Ratcliffe, E. H. *Philosophical Magazine* **1962**, *7*, 1197.

(12) Dillard, D. S.; Timmerhaus, K. D. *Low temperature thermal conductivity of selected dielectric crystalline solids. In Thermal conductivity-Proceedings of the eighth conference*; Plenum Press: New York, **1969**.

(13) Slack, G. A. *Phys. Rev. B* **1980**, *22*, 3065.

(14) Bertie, J. E.; Labbe, H. J.; Whally, E. *J. Chem. Phys.* **1969**, *50*, 4501.

(15) Wong, P. T. T.; Whalley, E. *J. Chem. Phys.* **1975**, *62*, 2418.

(16) Wong, P. T. T.; Whalley, E. *J. Chem. Phys.* **1976**, *65*, 829.

(17) Li, J. C.; Ross, D. K.; Londono, J. D.; Finney, J. L.; Kolesnikov, A.; Ponyatovskii, E. G. *Neutron scattering studies of ice dynamics. Part III-Inelastic incoherent neutron scattering studies of ice II, V, VI, VIII and IX. In Physics and chemistry of ice*; Hokkaido University Press: Sapporo, **1992**.

(18) Li, J. C. *J. Chem. Phys.* **1996**, *105*, 6733.

(19) Petrenko, V. F.; Chesnakov, V. A. *Fiz. Tverd. Tela* **1990b**, *32*, 2368.

(20) Bjerrum, N. *Matematisk-Fysiske Meddelelser Kongelige Danske Videnskabernes Selskab* **1951**, *27*, 1.

(21) Granicher, H. *Zeitschrift für Kristallographie* **1958**, *110*, 432.

(22) Girifalco, L. A. *Statistical physics of materials, Chap. 8*; Wiley: New York, **1973**.

(23) Kuhn, W.; Thurkauf, M. *Helv. Chim. Acta* **1958**, *41*, 938.

(24) Livingston, F. E.; Whipple, G. C.; George, S. M. *J. Chem. Phys.* **1998**, *108*, 2197.

(25) Neftel, A.; Moor, E.; Oeschger, H.; Stauffer, B. *Nature* **1985**, *315*, 45.

(26) Neftel, A.; Oeschger, H.; Staffelbach, T.; Stauffer, B. *Nature* **1988**, *331*, 609.

(27) Raynaud, D.; Chappellaz, J.; Barnola, J. M.; Korotkevich, Y. S.; Lorius, C. *Nature* **1988**, *333*, 655.

(28) Stauffer, B.; Lochbronner, E.; Oeschger, H.; Schwander, J. *Nature* **1988**, *332*, 812.

(29) Chappellaz, J.; Barnola, J. M.; Raynaud, D.; Korotkevich, Y. S.; Lorius, C. *Nature* **1990**, *345*, 127.

(30) Miller, S. L. *Science* **1969**, *165*, 489.

(31) Shoji, H.; Langway, C. C. *Nature* **1982**, *298*, 548.

(32) Ikeda, T.; Fukazawa, H.; Mae, S.; Pepin, L.; Duval, P.; Champagnon, B.; Lipenkov, V. Y.; Hondoh, T. *Geophys. Res. Lett.* **1999**, *26*, 91.

(33) Ikeda-Fukazawa, T.; Hondoh, T.; Fukumura, T.; Fukazawa, H.; Mae, S. *J. Geophys. Res.-Atmos.* **2001**, *106*, 17799.

(34) Ikeda-Fukazawa, T.; Hondoh, T. *Mem. Natl. Inst. Polar Res.* **2003**, 178.

(35) Satoh, K.; Uchida, T.; Hondoh, T.; Shinji, M. *Proc. NIPR Symp. Polar Meterol. Glaciol.* **1996**, *10*, 73.

(36) Goto, K.; Hondoh, T.; Higashi, A. *Jpn. J. Appl. Phys. Part 1 - Regul. Pap. Short Notes Rev. Pap.* **1986**, *25*, 351.

(37) Woafo, P.; Takontchoup, R.; Bokosah, A. S. *J. Phys. Chem. Solids* **1995**, *56*, 1277.

(38) Domine, F.; Thibert, E. *Relationship between atmospheric composition and snow composition for HCl and HNO_3* Wallington, 1995.

(39) Domine, F.; Thibert, E.; Silvente, E.; Legrand, M.; Jaffrezo, J. L. *J. Atmos. Chem.* **1995**, *21*, 165.

(40) Domine, F.; Thibert, E. *Geophys. Res. Lett.* ***1*998**, *25*, 4389.

(41) Sommerfeld, R. A.; Knight, C. A.; Laird, S. K. *Geophys. Res. Lett.* **1998**, *25*, 4391.

(42) Sommerfeld, R. A.; Knight, C. A.; Laird, S. K. *Geophys. Res. Lett.* **1998**, *25*, 935.

(43) Livingston, F. E.; Smith, J. A.; George, S. M. *Anal. Chem.* **2000**, *72*, 5590.

(44) Domine, F.; Xueref, I. *Anal. Chem.* **2001**, *73*, 4348.

(45) Livingston, F. E.; Smith, J. A.; George, S. M. *J. Phys. Chem. A* **2002**, *106*, 6309.

(46) Perrier, S.; Sassin, P.; Domine, F. *Can. J. Phys.* **2003**, *81*, 319.

(47) Warren, S. G. *Rev. Geophys.* **1982**, *20*, 67.

(48) Petrovich, D. K.; Govani, J. W. *Geophys. Res. Lett.* **1991**, *18*, 1233.

(49) Beaglehole, D.; Ramanathan, B.; Rumberg, J. *J. Geophys. Res.-Atmos.* **1998**, *103*, 8849.

(50) King, M. D.; Simpson, W. R. *J. Geophys. Res.-Atmos.* **2001**, *106*, 12499.

(51) Tyndall, J. *The glaciers of the Alps*; John Murray: London, **1860**.

(52) Hopkins, W. *Philos. Trans. R. Soc. London* **1862**, *152*, 677.

(53) Reusch, E. *Ann. Phys. Chem.* **1864**, *121*, 573.

(54) McConnel, J. C.; Kidd, D. A. *Proc. R. Soc. London* **1888**, *44*, 331.

(55) Glen, J. W.; Perutz, M. F. *J. Glaciol.* **1954**, *2*, 397.

(56) Taylor, G. I. *J. Inst. Met.* **1938**, *62*, 307.

(57) Groves, G. W.; Kelly, A. *Philos. Mag.* **1963**, *8*, 877.

(58) Hutchinson, J. W. *Metall. Trans. A* **1977**, *8*, 1465.

(59) Faraday, M. *Michael Faraday's Diary* **1833**, 79.

(60) Faraday, M. *Lecture before the Royal Institution reported in the Athaneum* **1850**, 640.

(61) Faraday, M. *Proc. R. Soc. London* **1860**, *10*, 152.

(62) Taylor; Francis *Experimental Researches in Chemistry and Physics* New York, **1991**.

(63) Dash, J. G.; Fu, H. Y.; Wettlaufer, J. S. *Rep. Prog. Physics* **1995**, *58*, 115.

(64) Dash, J. G. *Science* **1989**, *246*, 1591.

(65) Takagi, S. *J. Coll. Inter. Sci.* **1990**, *137*, 446.

(66) Golecki, I.; Jaccard, C. *J. Phys. C: Solid State Phys.* **1978**, *11*, 4229.

(67) Beaglehole, D.; Nason, D. *Surf. Sci.* **1980**, *96*, 357.

(68) Gilpin, R. R. *J. Colloid Interface Sci.* **1980**, *77*, 435.

(69) Elbaum, M.; Lipson, S. G.; Dash, J. G. *J. Cryst. Growth* **1993**, *129*, 491.

(70) Conklin, M. H.; Bales, R. C. *J. Geophys. Res.-Atmos.* **1993**, *98*, 16851.

(71) Dosch, H.; Lied, A.; Bilgram, J. H. *Surf. Sci.* **1996**, *366*, 43.

(72) Furukawa, Y.; Nada, H. *J. Phys. Chem. B* **1997**, *101*, 6167.

(73) Doppenschmidt, A.; Butt, H. J. *Langmuir* **2000**, *16*, 6709.

(74) Pittenger, B.; Fain, S. C.; Cochran, M. J.; Donev, J. M. K.; Robertson, B. E.; Szuchmacher, A.; Overney, R. M. *Phys. Rev. B* **2001**, *6313*, art. no.

(75) Bluhm, H.; Ogletree, D. F.; Fadley, C. S.; Hussain, Z.; Salmeron, N. *J. Phys.: Condens. Matter* **2002**, *14*, L227.

(76) Sadtchenko, V.; Ewing, G. E. *J. Chem. Phys.* **2002**, *116*, 4686.

(77) Abraham, F. F. *Rep. Prog. Phys.* **1982**, *45*, 1113.

(78) Phillips, J. M. *Phys. Lett. A* **1990**, *147*, 54.

(79) Hakkinen, H.; Manninen, M. *Phys. Rev. B* **1992**, *46*, 1725.

(80) Lowen, H. *Phys. Rep.-Rev. Sec. Phys. Lett.* **1994**, *237*, 249.

(81) Ohnesorge, R.; Lowen, H.; Wagner, H. *Phys. Rev. E* **1994**, *50*, 4801.

(82) Landa, A.; Wynblatt, P.; Hakkinen, H.; Barnett, R. N.; Landman, U. *Phys. Rev. B* **1995**, *51*, 10972.

(83) Wettlaufer, J. S. *Phys. Rev. Lett.* **1999**, *82*, 2516.

(84) Zhu, D. M.; Pengra, D.; Dash, J. G. *Phys. Rev. B* **1988**, *37*, 5586.

(85) Mulvaney, R.; Wolff, E. W.; Oates, K. *Nature* **1988**, *331*, 247.

(86) Nye, J. F. *J. Glaciol.* **1989**, *35*, 17.

(87) Fukazawa, H.; Sugiyama, K.; Mae, S. J.; Narita, H.; Hondoh, T. *Geophys. Res. Lett.* **1998**, *25*, 2845.

(88) Reynolds, O. *Papers on Mechanical and Physical Subjects*; Cambridge University Press: Cambridge, **1901**; Vol. 2.

(89) Bowden, F. P.; Hughes, T. P. *Proc. R. Soc. London A* **1939**, *172*, 280.

(90) Bowden, F. P. *Proc. R. Soc. London Ser. A-Math. Phys. Sci.* **1953**, *217*, 462.

(91) Evans, D. C. B.; Nye, J. F.; Cheeseman, K. J. *Proc. R. Soc. London Ser. A-Math. Phys. Eng. Sci.* **1976**, *347*, 493.

(92) Colbeck, S. C. *J. Glaciol.* **1988**, *34*, 78.

(93) Colbeck, S. C.; Warren, G. C. *J. Glaciol.* **1991**, *37*, 228.

(94) Turner, G. J.; Stow, C. D. *Philos. Mag. A-Phys. Condens. Matter Struct. Defect Mech. Prop.* **1984**, *49*, L25.

(95) Baker, M. B.; Dash, J. G. *J. Geophys. Res.-Atmos.* **1994**, *99*, 10621.

(96) Abbatt, J. P. D.; Beyer, K. D.; Fucaloro, A. F.; McMahon, J. R.; Wooldridge, P. J.; Zhang, R.; Molina, M. J. *J. Geophys. Res.-Atmos.* **1992**, *97*, 15819.

(97) Gross, G. W. *Adv. Chem. Series* **1968**, 27.

(98) Gross, G. W.; McKee, C.; Wu, C. H. *J. Chem. Phys.* **1975**, *62*, 3080.

(99) Gross, G. W.; Wong, P. M.; Humes, K. *J. Chem. Phys.* **1977**, *67*, 5264.

(100) Gross, G. W.; Gutjahr, A.; Caylor, K. *J. Physique* **1987**, *48*, 527.

(101) Dash, J. G.; Fu, H. Y.; Wettlaufer, J. S. *Rep. Prog. Phys.* **1995**, *58*, 115.

(102) Takenaka, N.; Ueda, A.; Daimon, T.; Bandow, H.; Dohmaru, T.; Maeda, Y. *J. Phys. Chem.* **1996**, *100*, 13874.

(103) Wolff, E. W. *Chemical exchange between the atmosphere and polar ice*; Springer-Verlag: Berlin, **1996**; Vol. I 43.

(104) Killawee, J. A.; Fairchild, I. J.; Tison, J. L.; Janssens, L.; Lorrain, R. *Geochim. Cosmochim. Acta* **1998**, *62*, 3637.

(105) Rempel, A. W.; Waddington, E. D.; Wettlaufer, J. S.; Worster, M. G. *Nature* **2001**, *411*, 568.

(106) Lodge, J. P.; Baker, M. L.; Pierrard, J. M. *J. Chem. Phys.* **1956**, *24*, 716.

(107) Grant, N. H.; Clark, D. E.; Alburn, H. E. *J. Am. Chem. Soc.* **1961**, *83*, 4476.

(108) Weatherburn, M. W.; Logan, J. E. *Clin. Chim. Acta* **1964**, *9*, 581.

(109) Bruice, T. C.; Butler, A. R. *J. Am. Chem. Soc.* **1964**, *86*, 4104.

(110) Butler, A. R.; Bruice, T. C. *J. Am. Chem. Soc.* **1964**, *86*, 313.

(111) Alburn, H. E.; Grant, N. H. *J. Am. Chem. Soc.* **1965**, *87*, 4174.

(112) Grant, N. H.; Alburn, H. E. *Biochemistry* **1965**, *4*, 1271.

(113) Grant, N. H.; Alburn, H. E. *Science* **1965**, *150*, 1589.

(114) Grant, N. H.; Alburn, H. E. *Nature* **1966**, *212*, 194.

(115) Grant, N. H.; Clark, D. E.; Alburn, H. E. *J. Am. Chem. Soc.* **1966**, *88*, 4071.

(116) Grant, N. H.; Alburn, H. E. *Arch. Biochem. Biophys.* **1967**, *118*, 292.

(117) Fennema, O. *Water relations of foods*; Academic Press: London, 1975.

(118) Hatley, R. H. M.; Franks, F.; Day, H. *Biophys. Chem.* **1986**, *24*, 187.

(119) Hatley, R. H. M.; Franks, F.; Day, H.; Byth, B. *Biophys. Chem.* **1986**, *24*, 41.

(120) Bronshteyn, V. L.; Chernov, A. A. *J. Cryst. Growth* **1991**, *112*, 129.

(121) Workman, E. J.; Reynolds, S. E. *Phys. Rev.* **1950**, *78*, 254.

(122) Zhou, X. L.; Beine, H. J.; Honrath, R. E.; Fuentes, J. D.; Simpson, W.; Shepson, P. B.; Bottenheim, J. W. *Geophysical Research Letters* **2001**, *28*, 4087.

(123) Logan, J. A. *J. Geophys. Res.* **1983**, *88*, 10785.

(124) Platt, U. *The Origin of Nitrous and Nitric Acid in the Atmosphere*; Springer-Verlag: New York, **1986**; Vol. G6.

(125) Whitlow, S.; Mayewski, P. A.; Dibb, J. E. *Atmos. Environ. A - General Topics* **1992**, *26*, 2045.

(126) Legrand, M. R.; Delmas, R. J. *Atmos. Environ.* **1984**, *18*, 1867.

(127) Legrand, M. R.; Kirchner, S. *J. Geophys. Res.-Atmos.* **1990**, *95*, 3493.

(128) Crutzen, P. J.; Heidt, L. E.; Krasnec, J. P.; Pollock, W. H.; Seiler, W. *Nature* **1979**, *282*, 253.

(129) Noxon, J. F. *Geophys. Res. Lett.* **1976**, *3*, 463.

(130) Dhar, N. R.; Ram, A. *J. Indian Chem. Soc.* **1933**, *10*, 125.

(131) McConnel, J. C. *J. Geophys. Res.* **1973**, *78*, 7812.

(132) Junge, C. E. *J. Geophys. Res.* **1963**, *68*, 3849.

(133) Galbally, I. E.; Roy, C. R. *Nature* **1978**, *275*, 734.

(134) Dahe, Q.; Zeller, E. J.; Dreschhoff, G. A. M. *J. Geophys. Res-Space Phys.* **1992**, *97*, 6277.

(135) Mayewski, P. A.; Lyons, W. B.; Spencer, M. J.; Twickler, M.; Dansgaard, W.; Koci, B.; Davidson, C. I.; Honrath, R. E. *Science* **1986**, *232*, 975.

(136) Wolff, E. W. *Nitrate in Polar Ice*; Springer-Verlag: New York, 1995; Vol. I30.

(137) Mayewski, P. A.; Legrand, M. R. *Nature* **1990**, *346*, 258.

(138) Neubauer, J.; Heumann, K. G. *Fresen. J. Anal. Chem.* **1988**, *331*, 170.

(139) Silvente, E.; Legrand, M. *Ice Core Studies of Global Biogeochemical Cycles, NATO ASI Ser., Ser. 1* **1995**, *30*, 225.

(140) Yang, Q. Z.; Mayewski, P. A.; Whitlow, S.; Twickler, M.; Morrison, M.; Talbot, R.; Dibb, J.; Linder, E. *J.Geophys. Res.-Atmos.* **1995**, *100*, 5113.

(141) Legrand, M.; Wolff, E. W.; Wagenbach, D. *Ann. Glaciol.* **1999**, *29*, 66.

(142) Hou, S. G.; Qin, D. H.; Ren, J. W. *Ann. Glaciol.* **1999**, *29*, 73.

(143) Mulvaney, R.; Wagenbach, D.; Wolff, E. W. *J. Geophys. Res.* **1998**, *103*, 11021.

(144) Zepp, R. G.; Hoigne, J.; Bader, H. *Environ. Sci. Technol.* **1987**, *21*, 443.

(145) Warneck, P.; Wurzinger, C. *J. Phys. Chem.* **1988**, *92*, 6278.

(146) Zellner, R.; Exner, M.; Herrmann, H. *J. Atmos. Chem.* **1990**, *10*, 411.

(147) Alif, A.; Boule, P. *J. Photochem. Photobiol. A-Chem.* **1991**, *59*, 357.

(148) Mark, G.; Korth, H. G.; Schuchmann, H. P.; vonSonntag, C. *J. Photochem. Photobiol. A-Chem.* **1996**, *101*, 89.

(149) Mack, J.; Bolton, J. R. *J. Photochem. Photobiol. A-Chem.* **1999**, *128*, 1.

(150) Strickler, S. J.; Kasha, M. *Molecular Orbitals in Chemistry, Physics and Biology*; Academic Press, **1964**.

(151) Maria, H. J.; McDonald, J. R.; McGlynn, S. P. *J. Am. Chem. Soc.* **1973**, *95*, 1050.

(152) Shuali, U.; Ottoleng.M; Rabani, J.; Yelin, Z. *J. Phys. Chem.* **1969**, *73*, 3445.

(153) Wagner, I.; Strehlow, H. *Z. Phys. Chemie. Neue Folge* **1980**, *123*, 1.

(154) Hoigne, J.; Bader, H.; Haag, W. R.; Staehelin, J. *Water Res.* **1985**, *19*, 993.

(155) Hoigne, J.; Bader, H. *Science* **1975**, *190*, 782.

(156) Honrath, R. E.; Peterson, M. C.; Guo, S.; Dibb, J. E.; Shepson, P. B.; Campbell, B. *Geophys. Res. Lett.* **1999**, *26*, 695.

(157) Jones, A. E.; Weller, R.; Wolff, E. W.; Jacobi, H. W. *Geophys. Res. Lett.* **2000**, *27*, 345.

(158) Ridley, B.; Walega, J.; Montzka, D.; Grahek, F.; Atlas, E.; Flocke, F.; Stroud, V.; Deary, J.; Gallant, A.; Boudries, H.; Bottenheim, J.; Anlauf, K.; Worthy, D.; Sumner, A. L.; Splawn, B.; Shepson, P. *J. Atmos. Chem.* **2000**, *36*, 1.

(159) Peterson, M. C.; Honrath, R. E. *Geophys. Res. Lett.* **2001**, *28*, 511.

(160) Davis, D.; Nowak, J. B.; Chen, G.; Buhr, M.; Arimoto, R.; Hogan, A.; Eisele, F.; Mauldin, L.; Tanner, D.; Shetter, R.; Lefer, B.; McMurry, P. *Geophys. Res. Lett.* **2001**, *28*, 3625.

(161) Honrath, R. E.; Lu, Y.; Peterson, M. C.; Dibb, J. E.; Arsenault, M. A.; Cullen, N. J.; Steffen, K. *Atmos. Environ.* **2002**, *36*, 2629.

(162) Dibb, J. E.; Arsenault, M.; Peterson, M. C.; Honrath, R. E. *Atmos. Environ.* **2002**, *36*, 2501.

(163) Beine, H. J.; Honrath, R. E.; Domine, F.; Simpson, W. R.; Fuentes, J. D. *J. Geophys. Res.* **2002**, *107*.

(164) Beine, H. J.; Domine, F.; Simpson, W.; Honrath, R. E.; Sparapani, R.; Zhou, X. L.; King, M. *Atmos. Environ.* **2002**, *36*, 2707.

(165) Beine, H. J.; Domine, F.; Ianniello, A.; Nardino, M.; Allegrini, I.; Teinila, K.; Hillamo, R. *Atmos. Chem. Phys.* **2003**, *3*, 335.

(166) Honrath, R. E.; Peterson, M. C.; Dziobak, M. P.; Dibb, J. E.; Arsenault, M. A.; Green, S. A. *Geophys. Res. Lett.* **2000**, *27*, 2237.

(167) Sumner, A. L.; Shepson, P. B. *Nature* **1999**, *398*, 230.

(168) Domine, F.; Shepson, P. B. *Science* **2002**, *297*, 1506.

(169) Dibb, J. E.; Talbot, R. W.; Munger, J. W.; Jacob, D. J.; Fan, S. M. *J. Geophys. Res.* **1998**, *103*, 3475.

(170) Chu, L.; Anastasio, C. *J. Phys. Chem. A.* **2003**, *107*, 9594.

(171) Abbatt, J. P. D. *Geophys. Res. Lett.* **1997**, *24*, 1479.

(172) Zondlo, M. A.; Barone, S. B.; Tolbert, M. A. *Geophys. Res. Lett.* **1997**, *24*, 1391.

(173) Lawrence, M. G.; Crutzen, P. J. *Tellus Ser. B-Chem. Phys. Meteorol.* **1998**, *50*, 263.

(174) Weinheimer, A. J.; Campos, T. L.; Walega, J. G.; Grahek, F. E.; Ridley, B. A.; Baumgardner, D.; Twohy, C. H.; Gandrud, B.; Jensen, E. J. *Geophys. Res. Lett.* **1998**, *25*, 1725.

(175) Allamandola, L. J.; Sandford, S. A.; Valero, G. J. *Icarus* **1988**, *76*, 225.

(176) Bernstein, M. P.; Sandford, S. A.; Allamandola, L. J.; Chang, S.; Scharberg, M. A. *Astrophys. J.* **1995**, *454*, 327.

(177) Bernstein, M. P.; Sandford, S. A.; Allamandola, L. J.; Gillette, J. S.; Clemett, S. J.; Zare, R. N. *Science* **1999**, *283*, 1135.

(178) Allamandola, L. J. *Abstr. Pap. Am. Chem. Soc.* **2000**, *220*, U406.

(179) Dworkin, L. P.; Deamer, D. W.; Sandford, S. A.; Allamandola, L. J. *Proc. Natl. Acad. Sci. U. S. A.* **2001**, *98*, 815.

(180) Ehrenfreund, P.; Bernstein, M. P.; Dworkin, J. P.; Sandford, S. A.; Allamandola, L. J. *Astrophys. J.* **2001**, *550*, L95.

(181) Elsila, J. E.; Gillette, J. S.; Zare, R. N.; Bernstein, M. P.; Dworkin, J. P.; Sandford, S. A.; Allamandola, L. J. *Abstr. Pap. Am. Chem. Soc.* **2001**, *221*, U540.

(182) Bernstein, M. P.; Dworkin, J. P.; Sandford, S. A.; Cooper, G. W.; Allamandola, L. J. *Nature* **2002**, *416*, 401.

(183) Deamer, D.; Dworkin, J. P.; Sandford, S. A.; Bernstein, M. P.; Allamandola, L. J. *Astrobiology* **2002**, *2*, 371.

(184) Sandford, S. A.; Bernstein, M. P.; Dworkin, J. P.; Cooper, G. W.; Allamandola, L. J. *Meteorit. Planet. Sci.* **2002**, *37*, A125.

(185) Dworkin, J. P.; Gillette, J. S.; Bernstein, M. P.; Sandford, S. A.; Allamandola, L. J.; Elsila, J. E.; McGlothlin, D. R.; Zare, R. N. An evolutionary connection between interstellar ices and IDPs? Clues from mass spectroscopy measurements of laboratory simulations. In *Space Life Sciences: Steps Toward Origin(S) Of Life*; Pergamon-Elsevier Science Ltd: Kidlington, **2004**; Vol. 33; pp 67.

(186) Hudson, R. L.; Moore, M. H. *Icarus* **2004**, *172*, 466.